IMPACT CRATERS

Earth and Moon impact flux increased at the end of the Paleozoic

Sara Mazrouei[1]*, Rebecca R. Ghent[1,2], William F. Bottke[3], Alex H. Parker[3], Thomas M. Gernon[4]

The terrestrial impact crater record is commonly assumed to be biased, with erosion thought to eliminate older craters, even on stable terrains. Given that the same projectile population strikes Earth and the Moon, terrestrial selection effects can be quantified by using a method to date lunar craters with diameters greater than 10 kilometers and younger than 1 billion years. We found that the impact rate increased by a factor of 2.6 about 290 million years ago. The terrestrial crater record shows similar results, suggesting that the deficit of large terrestrial craters between 300 million and 650 million years ago relative to more recent times stems from a lower impact flux, not preservation bias. The almost complete absence of terrestrial craters older than 650 million years may indicate a massive global-scale erosion event near that time.

The abundance of terrestrial craters with diameters (D) ≥ 20 km decreases substantially with age. A common assumption is that this loss is driven by erosive and tectonic processes operating over hundreds of millions of years. Unfortunately, it is challenging to quantitatively test this hypothesis with existing terrestrial data. An alternative is to estimate terrestrial crater loss rates by comparing Earth's crater record with the Moon's. Earth and the Moon have been struck by the same impactor population over time, but large lunar craters have experienced limited degradation over billions of years. An obstacle to performing this test has been obtaining accurate dates for large lunar craters.

We used an analysis of the thermophysical characteristics of lunar impact ejecta as measured with the Diviner thermal radiometer on NASA's Lunar Reconnaissance Orbiter (LRO) (*1*, *2*) to estimate the ages of lunar craters with D >10 km and younger than 1 billion years (Ga). The formation of large lunar craters excavates numerous ≥1m ejecta fragments onto the Moon's surface. These recently exposed rocks have high thermal inertia and remain warm during the lunar night relative to the surrounding lunar soils (called regolith), which have low thermal inertia. The nighttime temperatures were calculated from three of Diviner's thermal infrared channels. Rock abundance values, defined as the fractional coverage of a Diviner pixel by exposed meter-scale rocks (Fig. 1), were obtained, simultaneously with rock-free lunar regolith temperatures, by exploiting the fact that a mixture of lunar rocks and regolith produces a mixed spectral radiance and therefore different estimates of brightness temperature in each of the three thermal infrared channels (*1*).

Using these data, an inverse relationship between rock abundance in large crater ejecta and crater age has been demonstrated by calculating ejecta rock abundance values for nine "index" craters with independently determined ages (*2*). Young craters were found to have high rock abundance in their ejecta, whereas rock abundance decreases with increasing crater age, eventually becoming indistinguishable from the background for craters older than ~1 Ga. The breakdown of lunar rocks has most likely occurred at a steady rate over the past billion years through the constant influx of tiny impactors and the thermal effects of lunar day-night cycling (*3*). We derived a crater age–rock abundance regression function shown in Fig. 1 and fig. S1 (*3*).

We identified 111 rocky craters on the Moon with D ≥10 km between 80°N and 80°S, with ejecta blankets that have rock abundance values high enough to distinguish them from the background regolith (Fig. 2A and table S1). We used the 95th percentile rock abundance values ($RA_{95/5}$), which are those that separate the upper 5% from the lower 95% of RA values for a given crater's ejecta. We chose 10 km as a minimum size for this analysis because those craters have penetrated the surface regolith deeply enough to have excavated large blocks from the underlying bedrock. This approach minimizes the influence of variations in original

[1]Department of Earth Sciences, University of Toronto, Toronto, ON, Canada. [2]Planetary Science Institute, Tucson, AZ, USA. [3]Southwest Research Institute, Boulder, CO, USA. [4]School of Ocean and Earth Science, University of Southampton, Southampton, UK.
*Corresponding author. Email: sara.mazrouei.seidani@mail.utoronto.ca

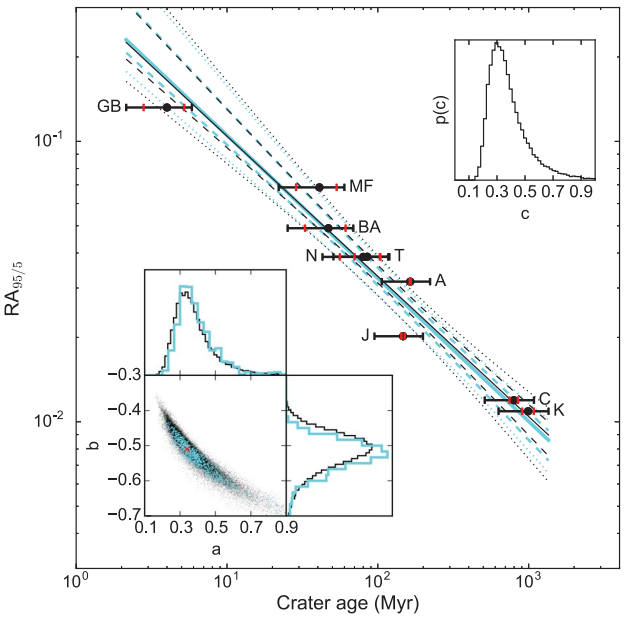

Fig. 1. Regression of lunar crater age versus 95th percentile rock abundance. Updated from (*1*, *2*). Data point labels correspond to dated lunar craters (*2*) listed in table S1. Rock cover is defined as materials with rocklike thermal inertia and minimum diameters larger than the diurnal thermal skin depth (~0.5 m). This regression differs from previous analysis (*2*) because of use of an updated rock abundance dataset and an updated age for Aristarchus crater (*26*), together with a statistical treatment that marginalizes over unacknowledged uncertainties for the published crater ages (*3*). Red error bars illustrate uncertainties for each crater, and black error bars show the uncertainties implied by the median value of the uncertainty scaling factor c given its posterior PDF (eq. S2). The best fitting parameters in the relation $RA_{95/5} = a \times (\text{age/Ma})^b$ are a, 0.33; b, −0.50 (black solid curve); black dashed and dotted curves indicate the 68 and 95% credible intervals. After propagation through the joint terrestrial/lunar Approximate Bayesian Computation rejection (ABCr) analysis (*3*), the best fitting parameters are a, 0.34; b, −0.51 (cyan solid curve); cyan dashed and dotted curves show the 68 and 95% credible intervals. (Insets) The two-dimensional (2D) distribution of the posterior PDF sample of parameters (a, b) before and after ABCr analysis (black and cyan points, respectively), their marginalized distributions, and $p(c)$, the 1D marginalized posterior PDF of the uncertainty scaling factor c (eq. S2).

Downloaded from http://science.sciencemag.org/ on January 28, 2019

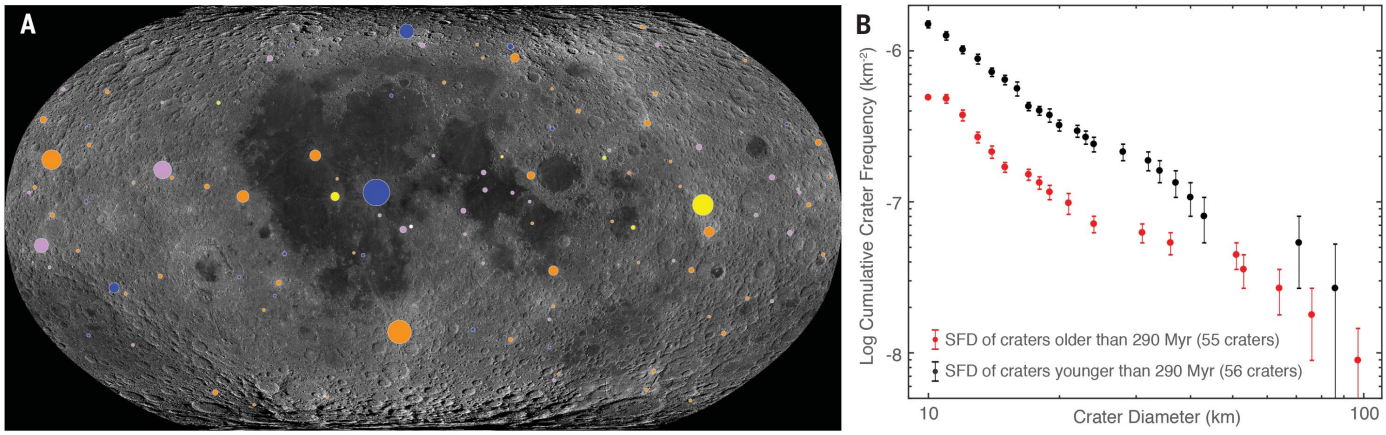

Fig. 2. Geographic and SFD of rocky lunar craters. (**A**) Geographic distribution of 111 rocky (young) craters with $D \geq 10$ km between 80°N and 80°S on the Moon (listed in table S1), scaled by size and color coded according to age. Orange (dark yellow deuteranopia) indicates craters younger than 290 Ma; pink (light blue deuteranopia) indicates craters 290 to 580 Ma old; dark blue indicates craters 580 to 870 Ma old; yellow indicates craters 870 to 1160 Ma old; and white indicates craters older than 1160 Ma. [Background image is from https://astrogeology.usgs.gov/search/map/Moon/LRO/LROC_WAC/Lunar_LRO_LROC-WAC_Mosaic_global_100m_June2013 (*27*)]. (**B**) Cumulative SFDs of craters. Red indicates average SFD of craters older than 290 Ma (55 craters; average of cumulative distribution in three age bins: 290 to 580 Ma old; 580 to 870 Ma old; and 870 to 1160 Ma old), black indicates craters younger than 290 Ma (56 craters), and error bars show Poisson noise. The lunar cratering rate has increased by a factor of 2.6 in the past 290 Ma compared with the preceding ~710 Ma.

ejecta block population that are due to spatial variations in surface soil thickness (*4*, *5*).

Using Fig. 1, we calculated ages for these craters and found that they were not formed uniformly with time (Fig. 2B). This implies that the small- and large-body impact fluxes striking the Moon are probably decoupled from one another at a modest level, with small impactors more likely to maintain a steady impact flux than large impactors (fig. S2) (*3*). Our analysis also showed no statistical evidence for a leading versus trailing hemisphere asymmetry in the calculated ages of these large craters, nor for a latitudinal dependence in rocky crater abundance, although our relatively small sample size might make such a trend difficult to detect. We also identified no correlation between crater sizes and crater ages, meaning differently sized craters are randomly distributed in time.

To quantify the change in flux exhibited by these lunar craters, we adopted a piecewise-constant rate model in which a uniform cratering rate at early times changes instantaneously to a different rate at later times. Sampling from among all possible values of the crater age–rock abundance regression parameters, using conservative estimates on the lunar index crater ages (Fig. 1) (*3*), we found that this model shows statistical evidence for a break at some time between 220 and 770 Ma ago (95% credible intervals), with the peak of the marginalized probability density function (PDF) at a break age of 400 Ma (fig. S1). The ratio of the crater rate after the break age to the prebreak rate is 2.1, with 95% credible interval values of 1.4 to 20.6.

Supporting evidence for an increase of a factor of 2 to 3 in the lunar impact flux since ~400 Ma ago may come from the ages and abundances of lunar impact spherules. Created by energetic cratering events, these glassy melt droplets have

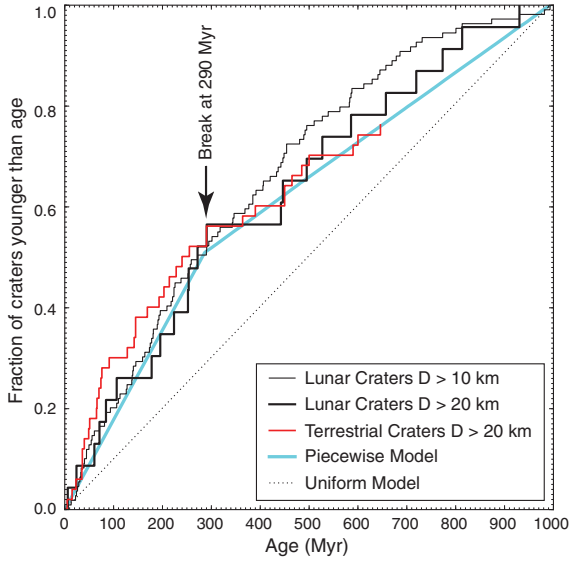

Fig. 3. Age-frequency distributions of lunar and terrestrial craters. The lunar crater $D \geq 10$ and 20 km curves are shown by the black line, whereas terrestrial craters with $D \geq 20$ km (table S2) are shown with the red line. All terrestrial craters are younger than 650 Ma. The lunar impact flux increases by a factor of 2.6 near 290 Ma ago (fig. S1). A simple piecewise model (cyan) demonstrates the break between two rates compared with a simple uniform model (dashed black). The similarity between the lunar and terrestrial distributions suggests that the inferred increase in terrestrial impacts is not a preservation bias.

been identified in the regolith samples returned from the Apollo landing sites. Their age distribution is a potential proxy for the impact flux of larger bodies and suggests that the impact flux increased by a factor of 3.7 ± 1.2 over the past 400 Ma (*6*, *7*), which is in broad agreement with our results. However, the abundance of young impact spherules found in Apollo lunar regolith samples could be a bias (*7*). Lunar craters formed over the past 300 to 400 Ma may have also degraded faster by means of diffusion processes than those that formed between 700 and 3100 Ma ago (*8*). This observation may be explained if large impacts enhance diffusive processes through, for example, seismic shaking, and the large-body impact flux has increased over recent times.

Rayed lunar craters have previously been used to compute impact flux rates, with the assumption often made that they formed in the past

Downloaded from http://science.sciencemag.org/ on January 28, 2019

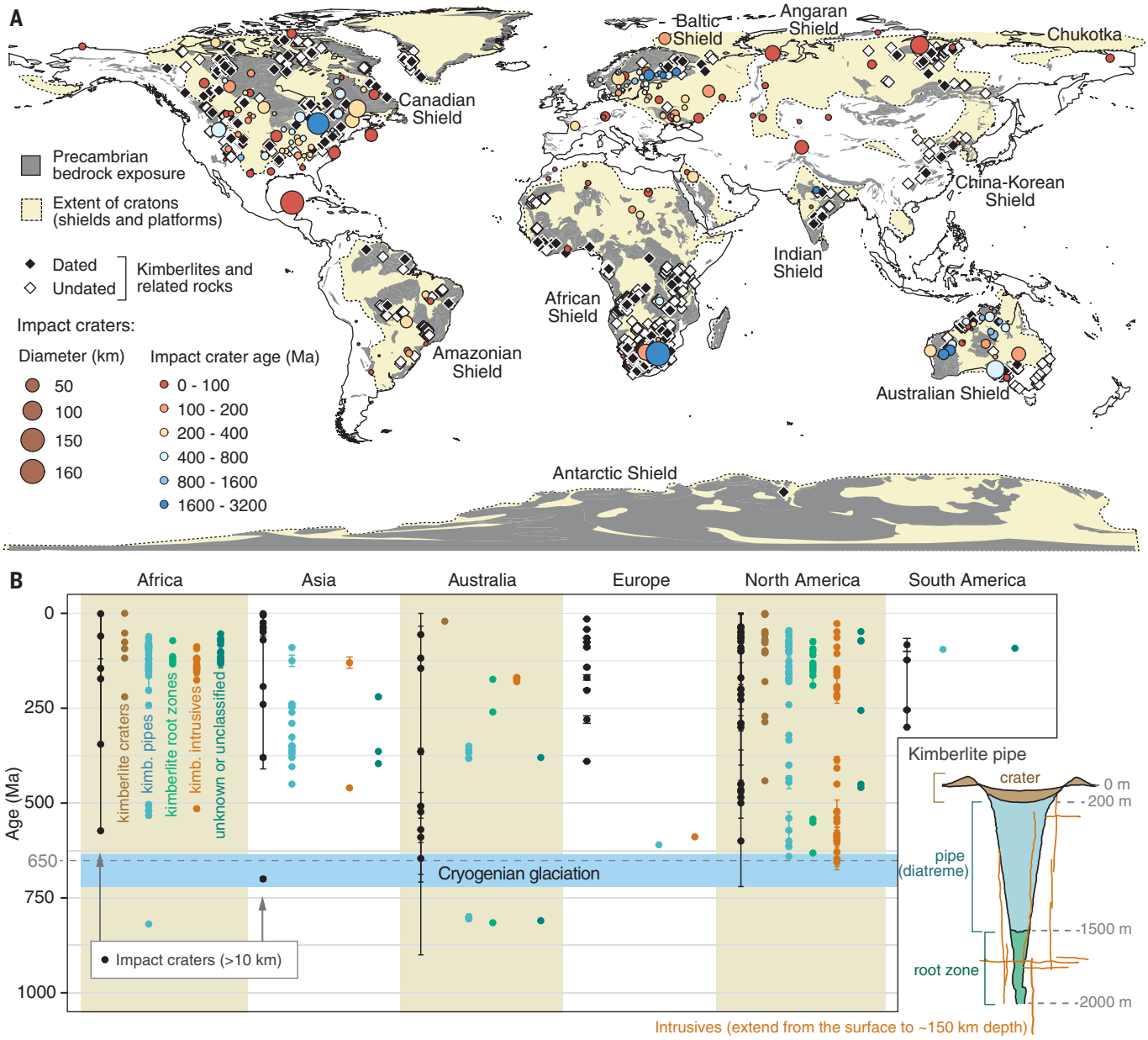

Fig. 4. Positions of terrestrial impact craters and kimberlites in space and time. (**A**) Locations of all impact craters identified in the Planetary and Space Science Centre (PASSC) Earth Impact Database (*24*), scaled by size and colored by age. Kimberlite occurrences are also shown; solid symbols denote those craters with well-defined ages (n = 624), and white diamonds indicate undated kimberlites (n = 3645) (*25*). Gray regions correspond to major exposures of Precambrian basement rocks (*28*), which together with platform areas shown in beige (*29*) form the stable cratons, where 84% of craters with $D \geq 20$ km (and 84.6% of craters with $D \geq 10$ km) occur. (**B**) Chronology of large impacts (>10 km) and well-dated kimberlites for each continent, excluding Antarctica. Colored symbols indicate depth-diagnostic kimberlite zones (labeled and illustrated in the inset). There is an abrupt cut-off in impact crater and kimberlite pipe frequency at ~650 Ma ago, which is coincident with Snowball Earth glaciation during the Cryogenian Period, 720 to 635 Ma ago (*17*–*19*).

1 Ga. We found 11 farside rocky craters with $D \geq$ 20 km formed in the past 1 Ga, compared with 28 to 32 farside rayed craters assumed to be this age (*9*, *10*). This discrepancy suggests that rayed craters may have a much wider spread of ages than commonly thought (supplementary text).

These results for the Moon provide insights into Earth's crater record. Interpretation of the terrestrial record is problematic because (i) an unknown number of older craters have been erased at unknown times by erosion or tectonics, (ii) stable continental surfaces capable of recording ancient impacts have potentially been buried and exhumed multiple times since they formed, (iii) it is difficult to precisely quantify which terrains have been adequately searched for craters, and (iv) not all craters are exposed at the surface but instead have to be identified through geophysical anomalies and explored through drilling (*11*).

Lunar craters have experienced comparatively little erosion over the past 1 Ga, and the proximity of Earth to the Moon implies that both have been struck by the same population of impactors. A comparison of records on both bodies therefore provides an opportunity to quantify terrestrial selection effects.

Downloaded from http://science.sciencemag.org/ on January 28, 2019

Contrary to our expectations, we found that the size-frequency distributions (SFDs) of the lunar and terrestrial craters for $D \geq 20$ km, normalized by the total number of craters, are highly similar (fig. S3A). We found no evidence for size bias in retention of terrestrial craters; in an average sense, for a given region, it appears that Earth either keeps all or loses all of its $D \geq 20$ craters at the same rate, independent of size.

We compared the ages of the 38 known terrestrial craters with $D \geq 20$ km (table S2) with the computed age distribution for lunar craters with $D \geq 10$ and ≥ 20 km (Fig. 3 and table S1). Using the same statistical method for the terrestrial craters as for the lunar craters, we found that the terrestrial craters also have a break age and ratio of present-day to past crater rate close to lunar values (fig. S1). Because there is evidence for a nonuniform terrestrial cratering rate similar to the lunar cratering rate, and considering that Earth and the Moon share a similar bombardment history, we combined both records. The inclusion of terrestrial craters provides an absolute age chronology supplement to the nine index craters we have for the Moon.

The model adopted to fit these data includes a single break between two uniform rates, but we do not rule out other simple models (for example, cratering rate linearly increasing in time) or more complex models (for example, multiple breaks). Rather, we used the single-break piecewise model as a simple and physically plausible hypothesis to demonstrate that the lunar and terrestrial cratering rates have not been constant over the past billion years.

Our joint lunar and terrestrial analysis yields a ratio of the crater rate after the break age to the prebreak rate of 2.6, with a 95% credible interval value of 1.7 to 4.7. The most probable break age is 290 Ma. The impact rate change is reflected in the SFD curves, with craters younger than 290 Ma substantially higher in frequency at all diameters than those older than 290 Ma (Fig. 2B). The deficit of large terrestrial craters between 290 and 650 Ma old can therefore be interpreted to reflect a lower impact flux relative to the present day and not a bias (supplementary text).

The erosion history of Earth's continents can also be constrained by using uranium-lead (U-Pb) thermochronology, or temperature-sensitive radiometric dating. Thermochronologic data suggest that stable continental terrains experience low erosion or burial rates of up to 2.5 m Ma^{-1} (*12*), which equates to a maximum of 1.6 km vertical erosion (or deposition) over the past 650 Ma. This would likely be insufficient to eradicate craters with $D \geq 20$ km, given that crater depths are approximately equal to ~10% of their original diameter (*13*).

Support for limited erosion on cratered terrains can also be found in the record of kimberlite pipes. Kimberlites are formed during explosive volcanism from deep mantle sources, generating carrot-shaped pipes 1 to 2 km deep (Fig. 4) (*14*, *15*), and commonly preserve volcanic features (such as volcanic craters and pipes) that are depth-diagnostic (*16*). Impact craters and kimberlites are frequently found in common regions on stable continental surfaces (Fig. 4A), so kimberlites are a proxy that indicate the depth of erosion for surfaces of different ages. Deep erosion of stable continental surfaces (>2 km) should have removed most kimberlite pipes, leaving behind deep-seated intrusive rocks, but kimberlite pipes are relatively common throughout the Phanerozoic Eon (541 Ma ago to the present). Their spatiotemporal distribution (Fig. 4B) suggests only modest erosion (<1 km) on most cratons since 650 Ma ago, favoring the survival of $D \geq 20$ km impact craters (*3*).

There is a sharp cut-off in the number of terrestrial craters at ~650 Ma ago (Figs. 3 and 4). Given erosion rates on stable continental terrains after 650 Ma ago, similar conditions further back in time would have allowed most craters of Precambrian age (older than 541 Ma) to survive. Instead, the paucity of Precambrian craters is coincident with major episodes of globally extensive "Snowball Earth" glaciation (Fig. 4B) (*17*). Pervasive subglacial erosion at ~650 to 720 Ma ago is thought to have removed kilometers of material from the continents (*18*, *19*), enough to erase most existing kimberlite pipes and impact craters (fig. S5A). The exceptions are the $D > 130$ km impact craters Sudbury (1850 Ma ago) and Vredefort (2023 Ma ago). Both craters were deep enough to survive, but each shows indications of multiple kilometers of erosion (*20*).

The change in the lunar and terrestrial impact flux may be due to the breakup of one or more large asteroids in the inner and/or central main asteroid belt (*21*). Those located near dynamical resonances may produce long-lived surges in the impact flux as the fragments are slowly driven to escape routes by nongravitational forces. Asteroid evolution models suggest that the contribution of kilometer-sized impactors from a large parent-body disruption would have reached their new level within a few tens of millions of years of the breakup event(s), with the wave of bodies perhaps receding after hundreds of millions of years (*21*, *22*).

REFERENCES AND NOTES

1. J. L. Bandfield *et al*., *J. Geophys. Res. Planets* **116**, E00H02 (2011).
2. R. R. Ghent *et al*., *Geology* **42**, 1059–1062 (2014).
3. Materials and methods are available as supplementary materials.
4. G. H. Heiken, D. T. Vaniman, B. M. French, *Lunar Sourcebook—A User's Guide to the Moon* (Cambridge Univ. Press, 1991).
5. R. J. Pike, *Geophys. Res. Lett.* **1**, 291–294 (1974).
6. T. S. Culler, T. A. Becker, R. A. Muller, P. R. Renne, *Science* **287**, 1785–1788 (2000).
7. N. Zellner, J. Delano, *Geochim. Cosmochim. Acta* **161**, 203–218 (2015).
8. C. I. Fassett, B. J. Thomson, *J. Geophys. Res. Planets* **119**, 2255–2271 (2014).
9. A. S. McEwen, J. M. Moore, E. M. Shoemaker, *J. Geophys. Res. Planets* **102** (E4), 9231–9242 (1997).
10. J. A. Grier, A. S. McEwen, P. G. Lucey, M. Milazzo, R. G. Strom, *J. Geophys. Res. Planets* **106** (E12), 32847–32862 (2001).
11. R. A. F. Greive, E. M. Shoemaker, The record of past impacts on Earth, in *Hazards Due to Comets and Asteroids* (Univ. Arizona Press, 1995), pp 417–462.
12. T. J. Blackburn *et al*., *Science* **335**, 73–76 (2012).
13. E. I. Smith, *J. Geophys. Res.* **76**, 5683–5689 (1971).
14. R. S. J. Sparks *et al*., *J. Volcanol. Geotherm. Res.* **155**, 18–48 (2006).
15. L. Wilson, J. W. Head Iii 3rd, *Nature* **447**, 53–57 (2007).
16. R. J. Brown, G. A. Valentine, *Geol. Soc. Am. Bull.* **125**, 1224–1238 (2013).
17. P. F. Hoffman, A. J. Kaufman, G. P. Halverson, D. P. Schrag, *Science* **281**, 1342–1346 (1998).
18. C. B. Keller *et al*., Neoproterozoic glacial origin of the Great Unconformity. *Proc. Natl. Acad. Sci. U.S.A.* 10.1073/pnas.1804350116 (2018).
19. M. S. DeLucia, W. R. Guenthner, S. Marshak, S. N. Thomson, A. K. Ault, *Geology* **46**, 167–170 (2017).
20. R. A. F. Grieve, W. U. Reimold, J. Morgan, U. Riller, M. Pilkington, *Meteorit. Planet. Sci.* **43**, 855–882 (2008).
21. W. F. Bottke, D. Vokrouhlický, D. Nesvorný, *Nature* **449**, 48–53 (2007).
22. D. Vokrouhlický, W. F. Bottke, D. Nesvorný, *Astron. J.* **153**, 172 (2017).
23. Paige *et al*., LRO DLRE LEVEL 5 GDR V1.0, NASA Planetary Data System, LRO-L-DLRE-5-GDR-V1.0 (2011); https://pds.nasa.gov/ds-view/pds/viewDataset.jsp?dsid=LRO-L-DLRE-5-GDR-V1.0; retrieved 22 July 2016.
24. "Earth Impact Database," Planetary and Space Science Centre (PASSC), University of New Brunswick; www.passc.net/EarthImpactDatabase; retrieved 22 July 2016.
25. S. Faure, CONSOREM Database (Version 3), Consortium de Recherche en Exploration Minérale CONSOREM, Université du Québec à Montréal; www.consorem.ca (2010); retrieved 22 July 2016.
26. M. Zanetti *et al*., *Icarus* **298**, 64–77 (2017).
27. H. Sato, M. S. Robinson, B. Hapke, B. W. Denevi, A. K. Boyd, *J. Geophys. Res. Planets* **119**, 1775–1805 (2014).
28. United States Geological Survey, Geologic Province Map; https://earthquake.usgs.gov/data/crust/type.html; retrieved 5 March 2018.
29. Geological Survey of Canada, "Generalized geological map of the world and linked databases," technical report 2915d (1995).

ACKNOWLEDGMENTS

We thank M. Schmeider and C. Koeberl for helpful discussions regarding ages of terrestrial craters, T. Hincks for her help generating the plots in Fig. 4 and fig. S5, and J. Husson for providing digital Precambrian bedrock outlines shown in Fig. 4. We thank P. F. Hoffman, C. B. Keller, and R. N. Mitchell for stimulating discussions concerning Cryogenian erosion. We also thank the anonymous referees for their useful and constructive comments. **Funding:** S.M.'s and R.R.G.'s work on this study were funded by a Discovery grant from the National Science and Engineering Research Council of Canada to R.R.G.; W.F.B.'s participation was supported by NASA's SSERVI program "Institute for the Science of Exploration Targets (ISET)" through institute grant NNA14AB03A. A.H.P.'s participation was supported in part by NASA's SSERVI program "Project for Exploration Science Pathfinder Research for Enhancing Solar System Observations (Project ESPRESSO)" through institute grant 80ARC0M0008. T.M.G. acknowledges funding from the UK Natural Environment Research Council, grant NE/R004978/1. **Author contributions:** R.R.G. conceived the lunar crater experiments and supervised data collection. S.M. collected lunar crater data. Statistical tests were performed by A.H.P. Expertise on asteroid evolution and impact probabilities was provided by W.F.B. Expertise on kimberlite pipes was provided by T.M.G. All authors (S.M, R.R.G., W.F.B, A.H.P., and T.M.G.) analyzed the results and wrote the manuscript. **Competing interests.** The authors have no competing interests. **Data and materials availability:** The LRO Diviner data used in this paper can be obtained from (*23*). The derived lunar crater data are provided in table S1, and the terrestrial crater data used [updated from (*24*)] are provided in table S2. The kimberlite database [updated from (*25*)] used to generate Fig. 4 and fig. S5 is provided in supplementary data file S1 (aar4058_s1). The Approximate Bayesian Computation rejection (ABCr) code and the counting area simulation code (used to generate fig. S4) are available at https://github.com/ghentr/Earth-Moon_flux.

SUPPLEMENTARY MATERIALS

www.sciencemag.org/content/363/6424/253/suppl/DC1
Materials and Methods
Supplementary Text
Figs. S1 to S6
Tables S1 and S2
References (*30*–*73*)
Data File S1

3 November 2017; resubmitted 5 June 2018
Accepted 5 December 2018
10.1126/science.aar4058

Downloaded from http://science.sciencemag.org/ on January 28, 2019

Science

Earth and Moon impact flux increased at the end of the Paleozoic

Sara Mazrouei, Rebecca R. Ghent, William F. Bottke, Alex H. Parker and Thomas M. Gernon

Science **363** (6424), 253-257.
DOI: 10.1126/science.aar4058

Impact rates on Earth and the Moon

The rate at which impacts produce craters on the Moon is used to calibrate ages in planetary science. Earth should also have received similar numbers of impacts, but many craters have been hidden by erosion, ice sheets, and so on. Mazrouei *et al.* used infrared images of the Moon to estimate the ages of young lunar craters (see the Perspective by Koeberl). They found that the impact rate increased within the past ~500 million years, a conclusion strengthened by an analysis of known impact craters on Earth. Crater size distributions are the same on Earth and the Moon over this period, implying that terrestrial erosion affects all craters equally, regardless of their size.

Science, this issue p. 253; see also p. 224

ARTICLE TOOLS http://science.sciencemag.org/content/363/6424/253

SUPPLEMENTARY MATERIALS http://science.sciencemag.org/content/suppl/2019/01/16/363.6424.253.DC1

REFERENCES This article cites 68 articles, 12 of which you can access for free
http://science.sciencemag.org/content/363/6424/253#BIBL

PERMISSIONS http://www.sciencemag.org/help/reprints-and-permissions

Use of this article is subject to the Terms of Service

Science (print ISSN 0036-8075; online ISSN 1095-9203) is published by the American Association for the Advancement of Science, 1200 New York Avenue NW, Washington, DC 20005. 2017 © The Authors, some rights reserved; exclusive licensee American Association for the Advancement of Science. No claim to original U.S. Government Works. The title *Science* is a registered trademark of AAAS.

Downloaded from http://science.sciencemag.org/ on January 28, 2019